



Surface defects decorated zinc doped gallium oxynitride nanowires with high photocatalytic activity



Jing Cheng, Yuting Wang, Yan Xing, Muhammad Shahid, Wei Pan*

State Key Laboratory of New Ceramics and Fine Processing, School of Materials Science and Engineering, Tsinghua University, Beijing 100084, PR China

ARTICLE INFO

Article history:

Received 28 October 2016

Received in revised form 2 February 2017

Accepted 1 March 2017

Available online 2 March 2017

Keywords:

Surface defects

Doping

Oxynitride

Electrospinning

Photocatalyst

ABSTRACT

It is known that surface defect is playing an important role in the photocatalytic performance. Defect engineering has become a common approach in the development of novel photocatalytic materials nowadays. In this paper, zinc doped gallium oxynitride nanowires enriched with surface defects are fabricated via a simple electrospinning and controlled calcination process under ammonia atmosphere. The surface defects are tuned by varying the ammonification temperature carefully, resulting in controlled doping content as well as adjustable crystallinity in the nanowire. The nanowire exhibits high photocatalytic activity and very good stability for the degradation of Rhodamine B organic dye. The apparent quantum efficiency reaches up to 30% under visible light irradiation, which is about 13 and 8 times higher than the nanowires with few surface defects. Structure analysis demonstrates that the surface oxygen vacancy is found to be the key factor for enhancing the photocatalytic efficiency. Hence, the enhanced photocatalytic activity can be attributed to the efficient charge transfer on the surface oxygen vacancy. The results in this work may be beneficial to explore the defective structure for the high performance visible-light driven photocatalytic materials for organic pollutant removal.

© 2017 Elsevier B.V. All rights reserved.

1. Introduction

Water pollution with various contaminations in lakes, rivers and aquifers, becomes a global environmental problem facing today's world. Purification of the sewage in most urban areas is also an urgent issue to the city residents and the environmental scientists. In the past decade, degradation of the organic contaminations by photocatalysts has been proved to be a sustainable water treatment process, and the development of novel and effective photocatalysts is still a hot topic at present. As a result, photocatalysts based on semiconductor materials have attracted much attention since the discovery of water splitting effect on a TiO_2 electrode by Fujishima and Honda in 1972 [1]. Since then, a plenty of researches concerned on semiconductor photocatalysts have been reported owing to the growing attention on environmental protection topics for water treatment and organic pollutant removal [2,3]. However, most of these materials can absorb light only in the ultraviolet range due to their wide band gaps. To efficiently utilize the solar energy, a lot of strategies have been developed to improve the photocatalytic activity under visible light irradiation. Among them, the oxyni-

trides raise great interest owing to their narrow bandgaps, suitable band structures and good stability [4,5]. Recently, since the discovery of zinc doped gallium oxynitride as a promising photocatalyst for overall water splitting by Domen et al. in 2005 [6], a lot of works have been conducted to achieve enhanced photocatalytic performance by bandgap engineering, co-catalysts modification, morphology design, and so on [7–11]. Lee et al. [12] have synthesized the material with a wide range of composition and the bandgap can get a minimum of 2.25 eV. Maeda et al. [13] have used the $\text{Rh}_{2-y}\text{Cr}_y\text{O}_3$ co-catalyst and achieved an apparent quantum efficiency of 5.9% at light wavelength range of 420–440 nm. Li et al. [14] have investigated the effect of the crystallographic facet on the oxynitride. Despite the improvement of the bandgap and co-catalyst design, there are still challenges remained to get high quantum efficiency of the zinc doped gallium oxynitride because the photogenerated carriers that can migrate to the surface are limited even with co-catalyst. Therefore, high efficiency zinc doped gallium oxynitride nanowires decorated by surface oxygen vacancies without co-catalyst are designed and prepared. In present study, we intended to tune the surface defects of the nanowires for optimized photocatalytic performance under visible light.

Generally, to enhance the photocatalytic performance, narrowing down the bandgap and enhancing the lifetime of electron-hole pairs are desired [15–17]. Doping is well known to introduce impu-

* Corresponding author.

E-mail address: panw@mail.tsinghua.edu.cn (W. Pan).

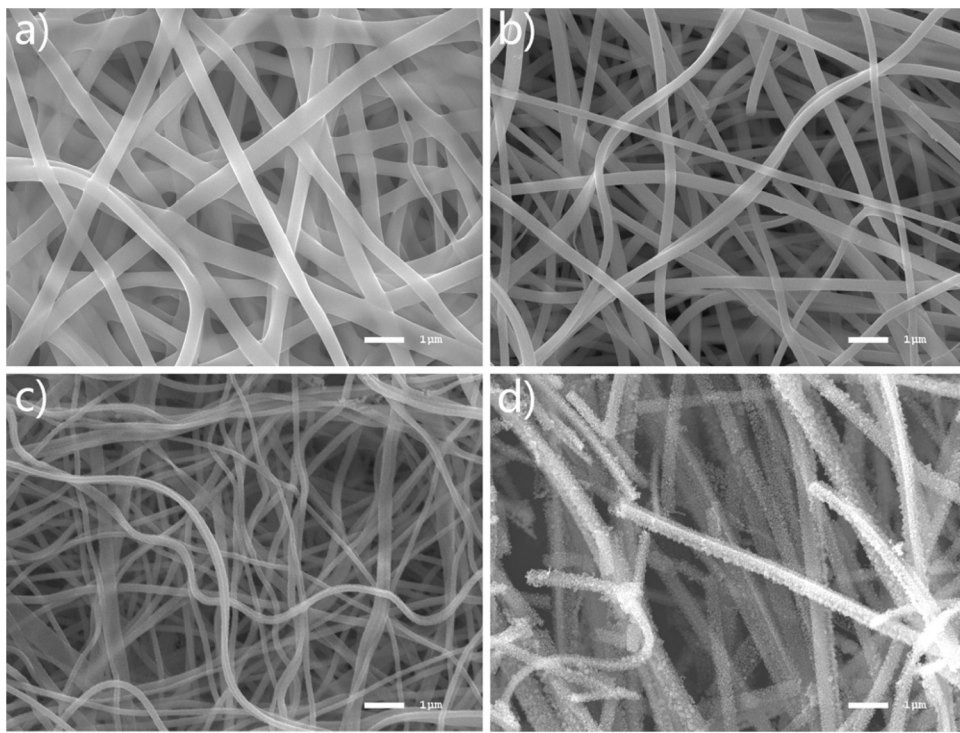


Fig. 1. SEM images of (a) as-spun nanowires and (b), (c), (d) the nanowires annealed at 700 °C, 800 °C, and 900 °C, respectively.

rities into a crystal structure, which may lead to the formation of defects in semiconductor materials. The lattice defects are found to have an effect on the electrical and optical properties significantly [18,19], and engineering the defects has been considered as an effective approach to adjust the bandgap of semiconductor materials [20]. In addition, surface defects are found to be the critical factor to improve the photocatalytic activity [21], which can trap the photogenerated electrons or holes and modify the phonon transport [22,23]. However, due to the complex structure and the uncertainty of surface chemical bonding condition, the effect of surface defects on the photocatalytic process has far from fully understood. Therefore, it is important to characterize the defects and reveal the effect of defects on the photoactivation and surface reactivity, which may help exploring novel materials for specific practical applications. Here, tunable surface defects in zinc doped gallium oxynitride nanowires are induced by doping and heat treatment process. The effects of surface defects on the photocatalytic activity are discussed accordingly.

In recent years, electrospinning is found to be a good method to prepare catalytic materials. The prepared ultrafine nanowires show good photocatalytic activity due to the merits of large surface-to-volume ratios [24]. The short electron-hole diffusion length to the surface of the nanowires can increase the lifetime of photogenerated electro-hole pairs, which is beneficial to the photocatalytic process [25]. Also, the electrospun nanowires have good recoverable character, as compared to nanopowders, the fibril photocatalysts can be easily separated and recycled from the solution [26].

In present study, zinc doped gallium oxynitride nanowires with high density of surface defects were synthesized by electrospinning and controlled heat treatment under ammonia flow. The phase structure and the morphology of the nanowires annealed at different temperature under ammonia atmosphere were determined. The surface chemical bonding state and photoluminescence properties has been studied. The photocatalytic efficiency was evaluated by the degradation of Rhodamine B (RhB) under visible light irradiation.

The mechanism of enhancement of photocatalytic efficiency under visible light exposure is discussed.

2. Experimental

2.1. Preparation of zinc doped gallium oxynitride nanowires

Zinc doped gallium oxynitride nanowires were prepared by the following procedure. Zinc acetate ($\text{Zn}(\text{Ac})_2 \cdot 2\text{H}_2\text{O}$) was dissolved in distilled water and then mixed well with Gallium nitrate solution ($\text{Ga}(\text{NO}_3)_3$, Ga 9–10 wt.%) and ethanol by magnetic stirring. Polyvinylpyrrolidone (PVP, MW = 1300 000) were then added to the solution. The weight ratio of the starting materials was $\text{Zn}(\text{Ac})_2 \cdot 2\text{H}_2\text{O}/\text{PVP}/\text{ethanol}/\text{H}_2\text{O} = 1/1/10/3.3$, and the mole ratio of gallium to zinc was 1:1. After complete dissolution, a clear transparent precursor solution was obtained. In a typical electrospinning procedure, the viscous solution was then put into a hypodermic syringe at a constant flow rate of 0.8 mL/h and then electrospun with an applied high voltage of 12.5 kV and an electrode distance of 15 cm, a grounded aluminum foil was used as the collector. The as-spun nanowires were calcined at 550 °C for 4 h to obtain the zinc doped gallium oxide (Ga-Zn-O) nanowires. To get the oxynitride, the obtained Ga-Zn-O precursor nanowires were then calcined under an ammonia atmosphere. In order to observe the structure change and get tunable content of defects, the calcination temperature was changed from 500 °C to 1000 °C, respectively, and the duration time was 4 h.

2.2. Photocatalytic reaction tests

The photocatalytic activity of the prepared nanowires was evaluated by the degradation of Rhodamine B (RhB) under visible light irradiation of a 300W Xe lamp with a 400 nm cutoff filter. The total optical power impinging on the solution was obtained as $100 \pm 10 \text{ mW/mL}$, measured by a digital power & energy meter (PM121D, Thorlabs Inc., Newton, NJ). The nanowires were dis-

persed in RhB solution (2.5×10^{-5} M, 10 mL) with a catalyst loading of 1 g/L. The mixture was magnetically stirred in the dark for 2 h to obtain the adsorption and desorption equilibrium of RhB and then loaded in an open beaker and exposed to irradiation with continuous stirring at room temperature. At regular intervals of 20 min, UV-vis absorption spectra of the separated solution were measured. The absorption at 554 nm referring to the concentration of RhB was recorded as a function of irradiation time.

2.3. Characterization

The morphology of the nanowires was characterized by scanning electron microscopy (SEM, JEOL JSM-6460LV, Tokyo, Japan) and transmission electron microscopy (TEM, JEOL-2011, Tokyo, Japan). The crystalline structure of the zinc doped gallium oxynitride nanowires was identified by X-ray diffraction (XRD, D/max-2550, Rigaku Co., Tokyo, Japan). X-ray photoelectron spectroscopy (XPS, PHI-5300 ESCA, PerkinElmer, Boston, MA) was measured for the analysis of elemental and chemical states in the nanowires. UV-vis diffuse reflectance spectra (UV-vis, Shimadzu, UV3600, Tokyo, Japan) were recorded under the diffuse reflectance mode in the scanning range of 300–800 nm. Photoluminescence spectra (PL, FLS-920, Edinburgh Instruments, Livingston, UK), electron spin-resonance spectroscopy (ESR, JEOL FA-200, Tokyo, Japan) and the effective surface area determination (BET, QuadraSorb Station 2, Florida, USA) were also measured.

3. Results and discussion

Fig. 1 shows the morphology of the Ga-Zn-O precursor and ammonification treated nanowires at different temperatures. The surface of the nanowires becomes a bit rougher as the temperature increased. The diameters of the nanowires are uniform but shrunk a little after the ammonification process.

The phase structures of the nanowires were studied by XRD. **Fig. 2a** shows the XRD patterns of the nanowires calcined at different temperature. The nanowires shows mono hexagonal wurtzite phase when the temperature is above 700 °C, indicating that a series of zinc doped gallium oxynitride with different doping contents have been successfully prepared. The existence of the mono phase can be further confirmed in **Fig. 2b** by the (101) peak, the peak shifts to higher degree from pure ZnO to pure GaN with the rise of the nitridation temperature. The *d* spacing of (101) becomes smaller as the ionic radius of Ga³⁺ is smaller than that of the Zn²⁺. We calculated the sizes of the crystals using Scherrer's formula, and found that the average crystal size changed as 11, 13, 17, 19, 26 nm, respectively, with the increase of nitridation temperature. It is demonstrated that the crystals in the electrospun zinc doped gallium oxynitride nanowires are still very fine even when the temperature is as high as 900 °C. The fine gain size can provide short electron-hole diffusion lengths to the interface and large interfacial surface areas.

High resolution transmission electron microscopy (HRTEM) images of the as prepared nanowires are shown in **Fig. 3**. It is demonstrated that the crystal size grows slightly as the temperature rises. The high resolution images show that the *d* spacing of 0.278 nm, 0.260 nm and 0.244 nm are in consistent with the (100), (002), and (101) lattice planes of wurtzite GaN and ZnO, which is in accord with the XRD results. The decrease of the *d* spacing can be further confirmed from the HRTEM results.

Table 1 shows the atomic ratios of the nanowires prepared at different nitridation temperatures, detected by EDS and XPS. A series of samples with different Zn contents are successfully prepared by tuning the nitridation temperature. In zinc doped gallium oxynitride, Zn and O are considered to randomly replace Ga and

Table 1

Atomic ratios and band gaps of zinc doped gallium oxynitride nanowires prepared at different nitridation temperatures.

Nitridation temperature/°C	Zn/(Zn+Ga) ratio (EDS)	Surface atomic ratio(XPS)		
		Zn/(Zn+Ga)	O/Ga	E _g /eV
700	0.43	0.45	1.57	2.74
750	0.43	0.36	1.23	2.70
800	0.12	0.10	1.10	3.05
850	0.10	0.07	1.27	3.11
900	0.07	0.02	0.95	3.27

N with short-range order [27]. Although the prepared nanowires exhibit a mono phase of wurtzite structure by XRD, doping could introduce lots of local lattice structure distortion because the ionic Zn-O bond is softer than the covalent Ga-N bond [27]. Thus, large amount of defects derived from local inhomogeneity are induced. Note that zinc interstitials, zinc vacancies, gallium interstitials, gallium vacancies, oxygen interstitials, oxygen vacancies, zinc antisites, gallium antisites and oxygen antisites, are likely to exist but the formation energies are really high for interstitials and antisites compared with the Gibbs formation energies of vacancies [28–31]. Moreover, the annealing in NH₃ ambient can further induce large amounts of surface defects such as dangling bonds, oxygen vacancies or zinc vacancies. The surface defects could be modified by the control of the doping level and the heat treatment process. To further investigate the behavior of zinc doping or rich vacancy defects on the nanowire surface, we have studied the chemical states of all the specimens by XPS analysis (**Fig. 4**).

The Ga 3d spectra (**Fig. 4a**) can be fitted in three symmetric peaks, referred to as Ga1, Ga2, and Ga3, where the peaks near 19.7, 20.4, and 19.2 eV correspond to Ga bonding to nitrogen (Ga-N, BE = 19.2–20.3 eV) [32], Ga bonding to oxygen (Ga-O, BE = 19.6–21 eV) [33], and Ga bonding to N-H (Ga-N-H, BE = 19.21 eV) [34]. The result indicates that the oxygen species exist not only around Zn atoms but also Ga atoms on the nanowire surface. As the temperature increases, the content of Ga-O bonding on the surface increases. In **Fig. 4b**, the core level spectrum of the Zn 2p_{3/2} region shows a symmetric peak centered around 1021 eV, which is lower than the energy position of ZnO (1022.4 eV) [35]. From the bond polarities of the Zn–O and Zn–N bonds, it is suggested that Zn–N bond is formed in the zinc doped gallium oxynitride. Note that the diffraction peaks of Zn 2p_{3/2} slightly shift to lower binding energy with the increase of nitridation temperature, which can be attributed to the increasing density of the Zn–N bond or the influence of the Zn–O–Ga bonding. **Fig. 4c** displays the N 1s spectra of all the prepared samples. The N 1s spectra can be fitted with four components: N1, N2, and two Ga LMM Auger electrons [36]. The N1 peak is corresponding to the N bonding to gallium (N–Ga, BE = 396.2–397.86 eV) [33], while N2 at around 398 eV is accord with the N bonding to hydrogen (N–H, BE = 397.7–399.72 eV) [37]. There is no sign of N–O type species to be found in XPS analysis results (above 405 eV) [38]. The diffraction peak of N–Ga shifts to higher degree as the zinc content decreases, indicating the tendency of the component changing to pure GaN at high temperature due to the loss of Zn at high temperature.

As shown in **Fig. 4d**, the spectra of O 1s can be divided into three peaks: O1, O2, and O3. The peaks near 530.4, 531.5, and 533 eV correspond to the binding energy of lattice oxygen, oxygen defects, and absorbed oxygen species, respectively [39]. It can be seen that large amounts of oxygen vacancies are introduced on the surface of the zinc doped gallium oxynitride nanowire. The O 1s peaks for the nanowires become much broaden and can be fitted by Gaussian distribution with three peaks. The intensity of the three peaks is affected by the nitridation temperature. It is noteworthy that the

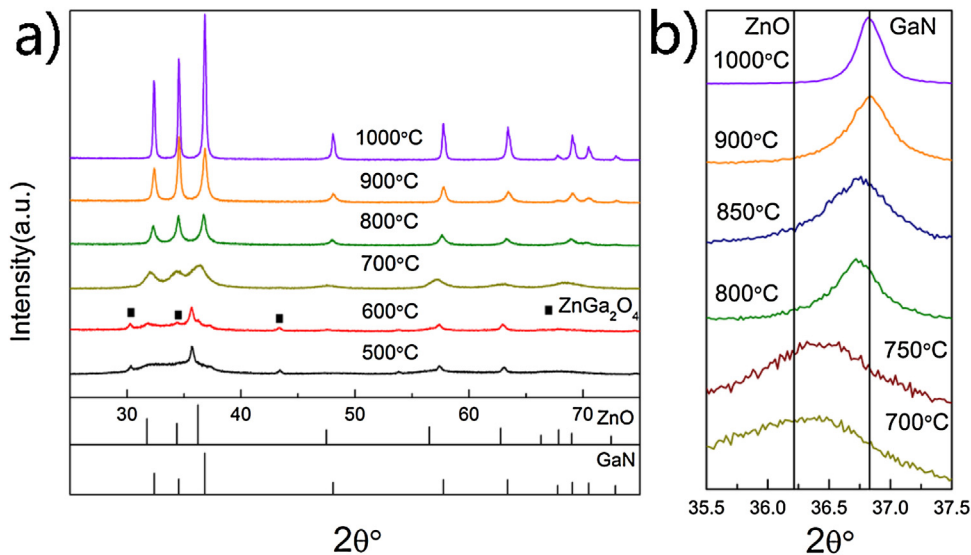


Fig. 2. XRD patterns of samples calcined at different temperatures.

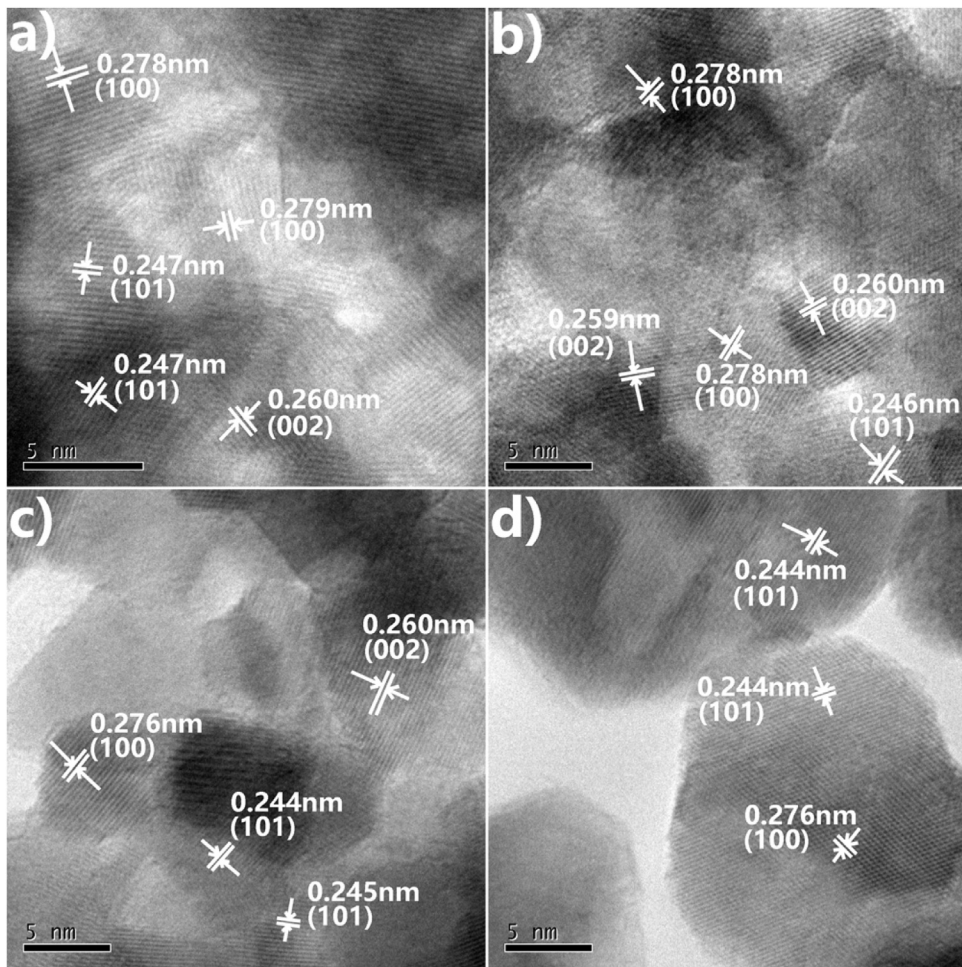


Fig. 3. HRTEM images of the nanowires calcined at different temperatures: (a) 750 °C; (b) 800 °C; (c) 850 °C, and (d) 900 °C.

medium binding energy component, centered at 531.5 eV, is connected to the variations in the concentration of oxygen vacancies. Therefore, we can estimate the concentration of surface oxygen vacancies according to the photoelectron cross-sections and the mean path. The intensities of this peak are shown in Table 2. For

nanowire calcined at 850 °C, the intensity of the peak at 531.5 eV is obviously stronger than that of the others, while the area ratio of the peak at 531.5 eV to the one at 530.4 eV is about 1.25, and the same ratio is only 0.72 in the nanowire calcined at 700 °C. It suggests that the oxygen vacancies in the fibrous surface region are

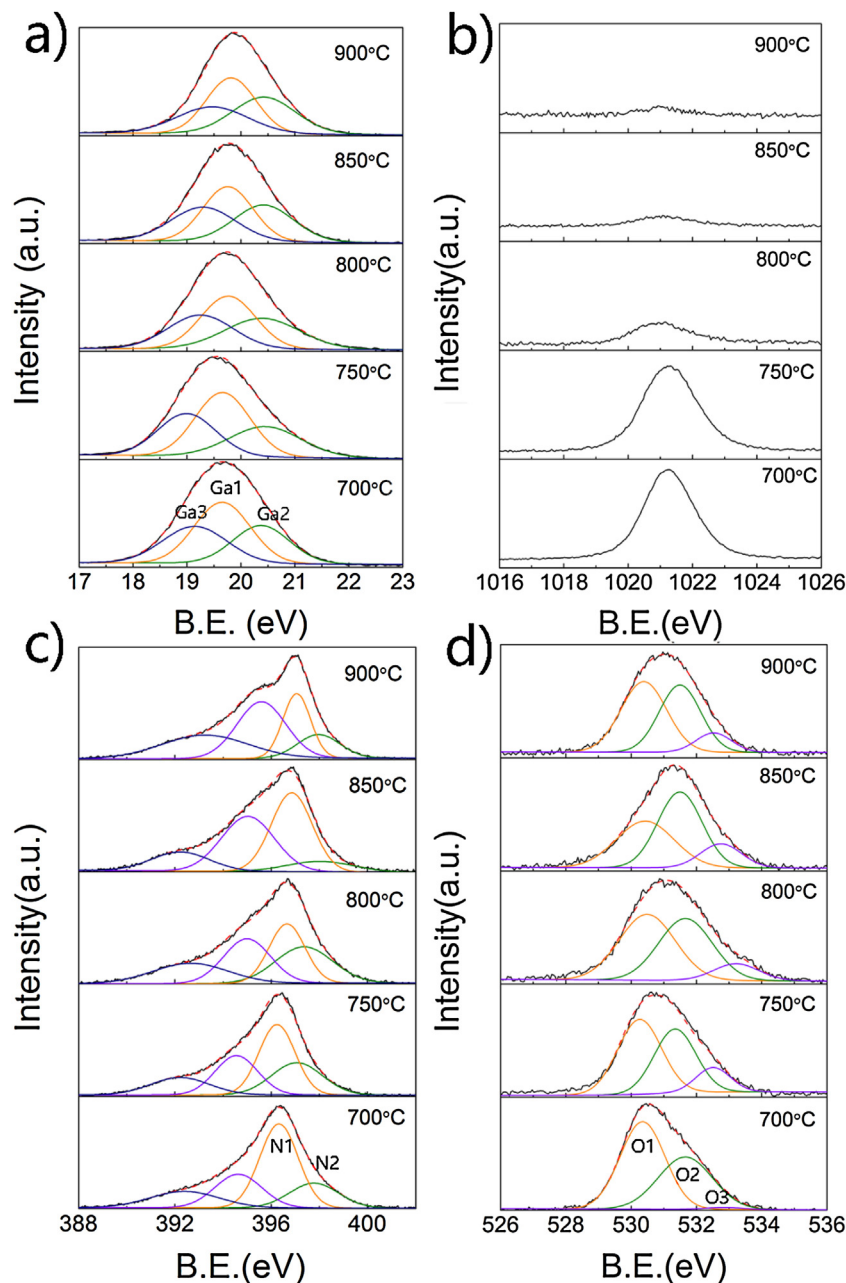


Fig. 4. XPS spectra of the nanowires calcined at different temperatures. (a, b, c, d) Ga 3d, Zn 2p, N 1s, and O 1s scan, respectively. The black solid lines are the experimental data, whereas the red dotted lines and thin lines are the fitting results. (For interpretation of the references to colour in this figure legend, the reader is referred to the web version of this article.)

Table 2
Details of the XPS peak information.

Peak Position (eV)	The area ratio of different peaks				
	700 °C	750 °C	800 °C	850 °C	900 °C
530.4	1	1	1	1	1
531.5	0.72	0.81	0.90	1.25	0.86
533.0	0.02	0.25	0.20	0.36	0.21

increased first and then decreased as the doping level decreases and the nitridation temperature increases while annealing under NH₃ atmosphere.

The solid-state ESR experiment has also been conducted to detect the defect state in the nanowire. Fig. 5 shows the ESR spectra of zinc doped gallium oxynitride at room temperature. A broad

peak at g factor of 2.004 is observed, which is corresponded to the overlap of different ESR signals belonging to singly ionized oxygen vacancies (V_O^{+}) and singly ionized Zn vacancy (V_{Zn}^{-}) [40]. Referred with the XPS results, we can see that the defects such as Zn vacancies and oxygen vacancies are existed in the nanowires. Moreover, the intensity of the ESR signal decreases as the temperature increases, indicating fewer bulk defects compared with the surface region. Thus, zinc doped gallium oxynitride nanowires with tunable surface defects are confirmed.

The photocatalytic performances of the nanowires with different ratio of surface defects have been evaluated by the degradation of RhB under visible light irradiation ($\lambda = 400\text{--}750\text{ nm}$). Catalyst loading of the nanofibers was 1 g/L. The total optical power (TOP) impinging on the sample was $100 \pm 10\text{ mW/mL}$. The specific surface area of the nanofibers measured using BET test is $35.55 \pm 3.92\text{ m}^2/\text{g}$.

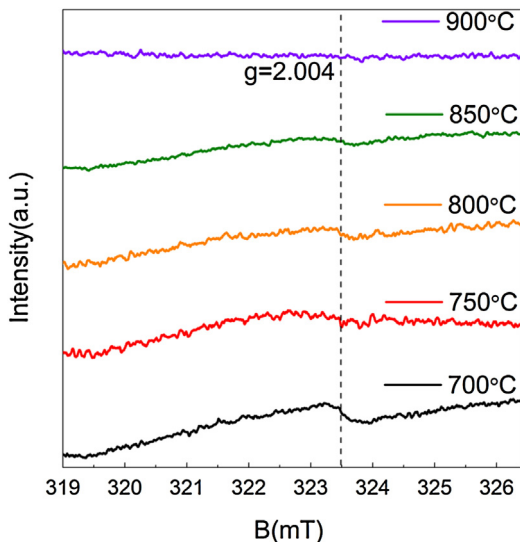


Fig. 5. ESR spectra of the nanowires calcined at different temperatures.

The normalized optical density change of RhB at the maximal absorption peak 554 nm is plotted in Fig. 6a as a function of time, and it is found that the optimal nitridation temperature is 850 °C. It is demonstrated in Fig. 6b that RhB is almost completely degraded when irradiated under visible light for 100 min. The color of RhB solution becomes clear (inset of Fig. 6b). It is known that the photodegradation of RhB can be considered as a pseudo-first-order

reaction [41,42]. The rate constant k can be calculated by the formula as follows:

$$C = C_0 e^{-kt} \quad (1)$$

Where t is the reaction time, C_0 and C are the RhB concentrations at initial and reaction time t , respectively. The photocatalytic activity of the zinc doped gallium oxynitride nanowires is strongly influenced by the nitridation temperature, shown in Fig. 6c. The nanowires calcined at 850 °C exhibit the highest photocatalytic activity with the rate constant k of 0.058 min⁻¹, which is more than 40 times of the nanowires calcined at 600 °C (0.001 min⁻¹). Obviously, the nanowire shows the catalytic activity under visible light. The apparent quantum efficiency (AQE) is defined as follows [43,44]:

$$AQE = \frac{d[x]/dt}{d[h\nu]_{inc}/dt} = \frac{kC_0}{TOP} \quad (2)$$

where $d[x]/dt$ is the initial rate of change of the concentration of the reactant, here for the degradation of RhB $d[x]/dt = kC_0$. $d[h\nu]_{inc}/dt$ is the total optical power (TOP) impinging on the sample. As the catalyst loading of the nanowire is 1 g/L, the TOP impinging on the nanowires is 0.016 ± 0.002 mW/mL. Based on the experimental data, the apparent quantum efficiency (AQE) is estimated by formula 2 and plotted in Fig. 6c. The AQE of the nanowire calcined at 600 °C (ZnO and ZnGa₂O₄ phases) is 0.6% and the one that calcined at 1000 °C (almost pure GaN phase) is 3.6%, while the AQE of the zinc doped gallium oxynitride calcined at 850 °C can reach as high as 29.4%. Here, AQE depends on the incident photons instead of the photons absorbed by the catalyst, so the real quantum yields

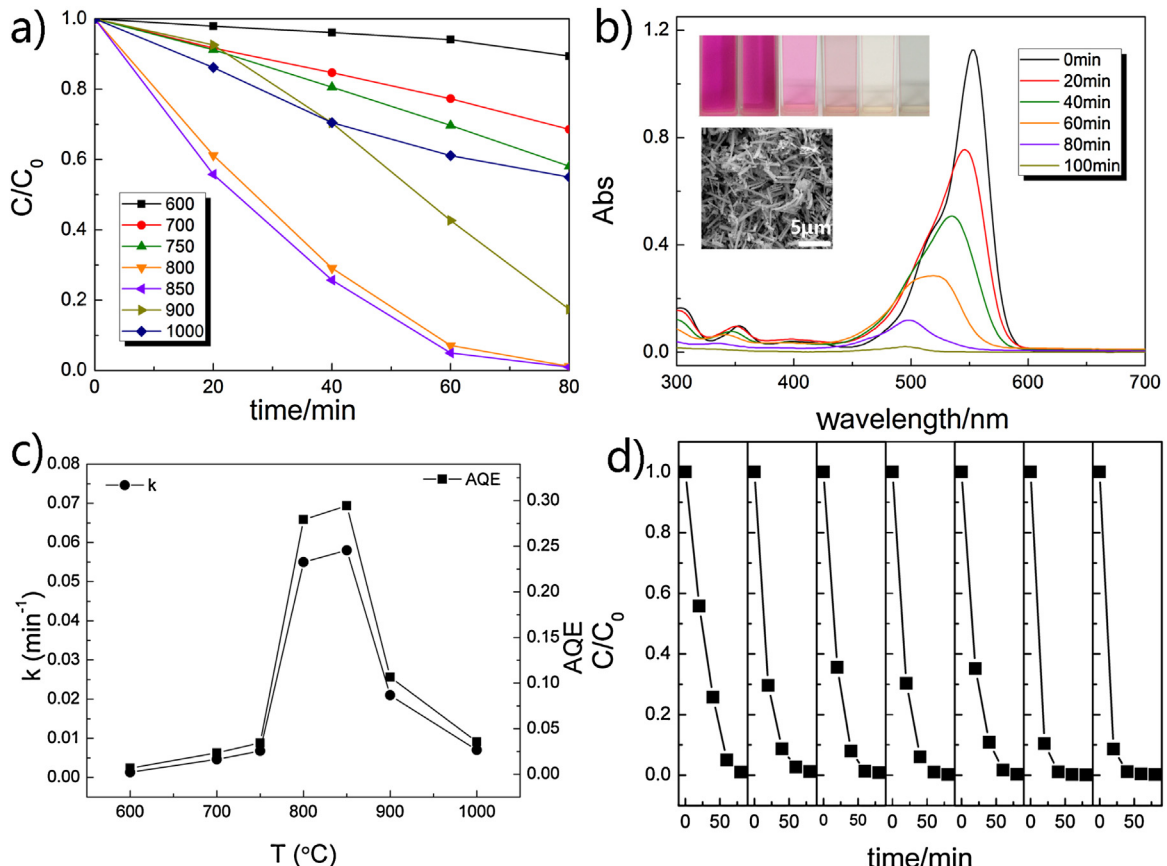


Fig. 6. (a) Photodegradation of RhB by zinc doped gallium oxynitride nanowires calcined at different temperatures; (b) The absorption spectrum of the RhB solution in the presence of the nanowires, the inset illustrates photos for the RhB solutions photodegraded with different time and the SEM image of the specimen reclaimed after photocatalytic measurement. (c) Degradation rate constants and apparent quantum efficiencies for the nanowires; (d) The repeatability tests of the specimen calcined at 850 °C.

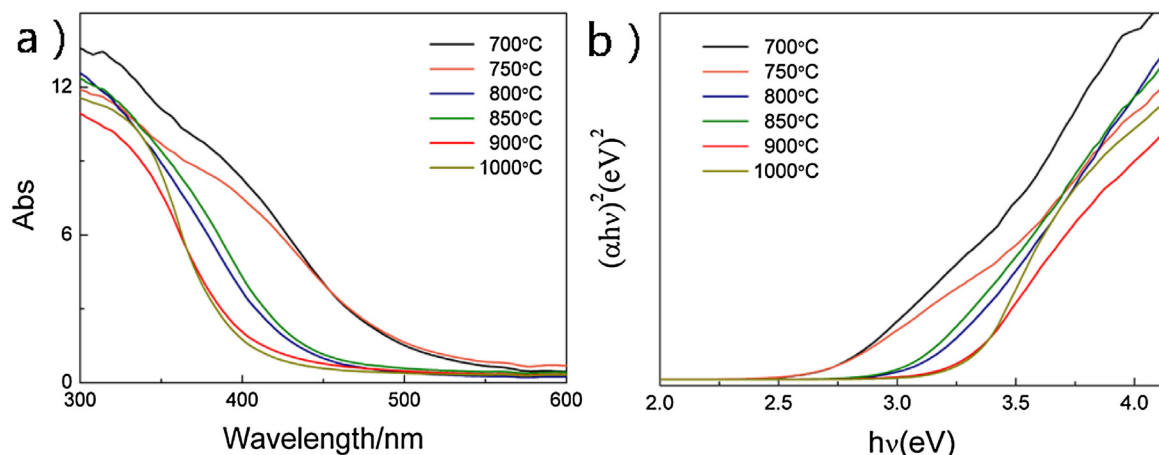


Fig. 7. (a) UV-vis diffuse reflection spectra of the nanowires calcined at different temperatures (b) the corresponding plots of $(\alpha h v)^2$ vs. photon energy ($h v$).

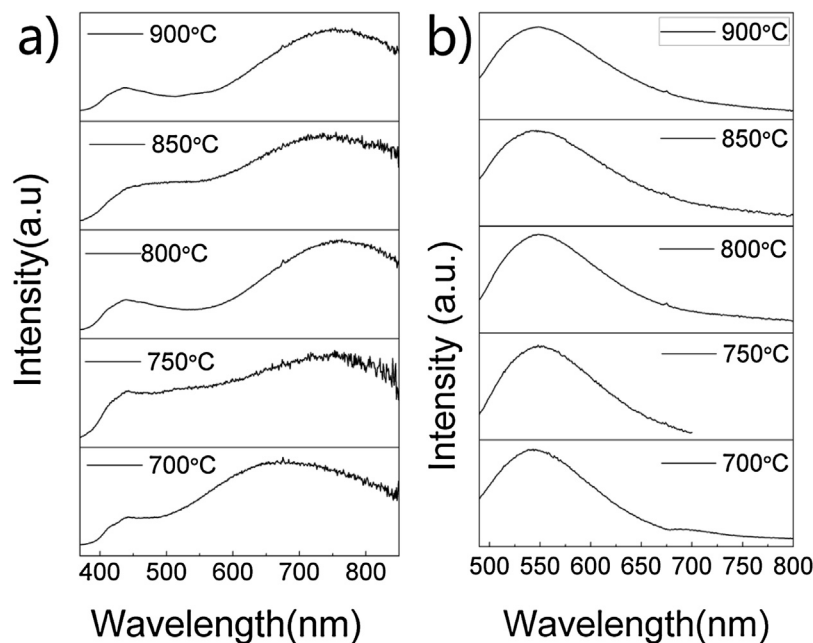


Fig. 8. Photoluminescence spectra at room temperature for zinc doped gallium oxynitride nanowires under excitation a) 346 nm and b) 466 nm, respectively.

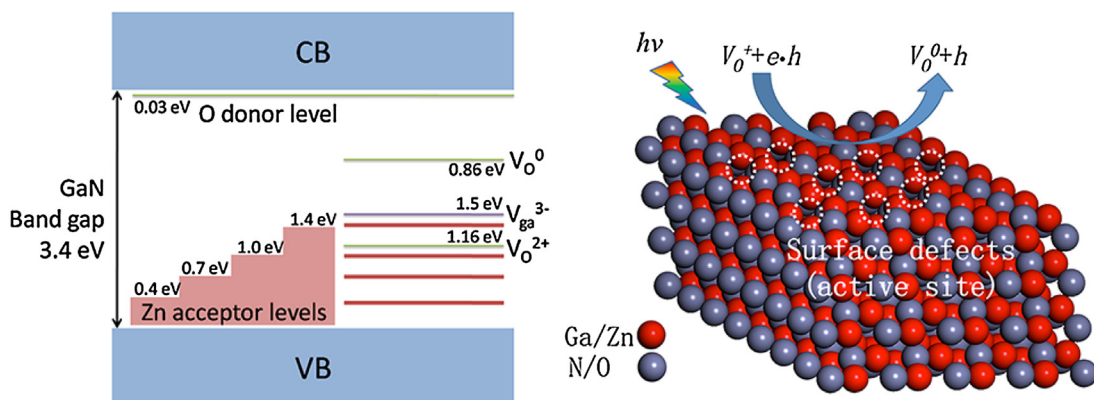


Fig. 9. Schematic illustrations of the surface defects related photocatalytic mechanism for zinc doped gallium oxynitride nanowires.

maybe higher than the value measured in this paper. The photocatalytic activity of the nanowires calcined at 850 °C also shows very good stability in the cyclic test (Fig. 6d). RhB can still be com-

pletely degraded under irradiation of visible light in 100 min after 7 cycle tests. The RhB adsorbed on the surface of the nanowire also proved to be removed totally after the cycle tests (see FT-IR results,

Supporting Information Fig. S1). The catalyst removed from the solution still shows the three-dimensional open structure although some nanowires broke into small pieces during the centrifugal process (inset of Fig. 6b). The nanowire shows good repeatability and stability.

Unlike the defects in the bulk, which act as the recombination center of the photogenerated electrons and holes, the surface defects are well known to enhance photocatalytic activity, which can increase the optical absorption of the light and serve as intermediate steps for the photo excitation process [45,46]. The charged oxygen vacancies are beneficial for electron transfer, contributing to a significant increase in photocatalytic performance. Thus, in present study, the nanowire calcined at 850 °C with high density of surfaces defects demonstrates the best photocatalytic performance. The high density of the surface oxygen vacancies can be attributed to the co-effect of zinc doping and the ammonia reduction.

From the band structure point of view, we have studied the photocatalytic mechanism of zinc doped gallium oxynitride enriched with surface defects in the visible light range. Fig. 7a shows the UV-vis diffuse reflection spectra of the nanowires calcined at different temperatures. The band gap can be estimated by the following formula [47]:

$$(\alpha h\nu)^2 = A(h\nu - E_g) \quad (3)$$

where, α is the absorption coefficient, h is the Planck's constant, ν is the incident light frequency, A is a constant, and E_g is the band gap, respectively. Therefore, the band gap of the nanowire can be estimated from data shown in Fig. 7b. The estimated E_g results are 2.74, 2.70, 3.05, 3.11 and 3.27 eV when calcination temperature changed from 700 to 900 °C, respectively, seen in Table 1. The band gap of the specimens is narrower than that of pure GaN (3.4 eV) and ZnO (3.2 eV) at low nitridation temperature but higher than that reported in literature [25]. High temperature leads to less Zn content because ZnO is easily volatilized when exposed to the ammonia atmosphere at high temperature. The band gap decreases as Zn content increases. The narrowed band gap most likely originates from the p-d (Zn 3d and N 2p) repulsion in the upper valence band [48]. Different zinc doping content affects the band gap of the nanowire. Although the nanowires calcined at 700 °C has good absorption of visible light, the photocatalytic activity is not so good. Because the intensity of the surface defects is low, while the ratio of bulk defects in the nanowire are high which result in poor photocatalytic activity. When the temperature is higher, zinc volatilizes and more surface defect are formed on the surface. But when zinc content further decreases, the structure of the nanowire tend to be pure GaN, the intensity of the surface defects decreases and absorption of the nanowire in the visible light range decreases. As a result, the photocatalytic activity of the nanowire calcined at 900 °C are relatively low. The nanowire calcined at 850 °C owns the highest density of the surfaces oxygen vacancies and good absorption in visible light range, resulting in the best photocatalytic performance.

To further confirm the effect of defects on the optical properties and investigate the origin of the visible light absorption of the nanowire, photoluminescence (PL) spectrum was characterized.

The PL spectra for the five specimens, obtained at room temperature under excitation at 346 nm, are shown in Fig. 8a. Broad PL bands are observed for all specimens. The broad PL bands appear to be comprised of several narrower bands, near 450 nm, 550 nm, and 700 nm, which are consistent with previous reports [49]. The photoluminescence excitation spectra (PLE) spectra of the prepared specimen do not shift with zinc composition (Fig. S2), which means that the change of intrinsic absorption edges of the nanowires is insignificant. In zinc doped gallium oxynitride, Zn is considered to be a substitution atom for Ga, corresponding to four acceptor levels [50]. As shown in Fig. 9, Zn-related acceptor levels are 0.4,

0.7, 1.0 and 1.4 eV above the valence band, resulting in four distinct PL bands with peaks at around 430, 480, 560 and 690 nm, respectively. This is further confirmed by the PL spectra under excitation of 466 nm at room temperature, see in Fig. 8b. Electrons are derived from level 0.7 eV and undergo radiative recombination with holes bound to 1.0 eV level. Oxygen substituted for N is likely to function as a donor element. The binding energy has been reported to be about 30 meV [51]. N rich condition favors the formation of gallium vacancy. The gallium vacancy is an acceptor like defect, which acts as a compensating center [50]. The formation energy of V_{Ga}^{3-} is relatively low when the Fermi level is close to the conduction band. The gallium vacancy is known to be the reason of the yellow luminescence of GaN [52]. Moreover, V_{Ga}^{3-} can capture the photogenerated holes, thereby delaying the recombination process. From the XPS results, it is indicated that there are large numbers of oxygen vacancy on the surface. In general, oxygen vacancy exists as V_O^+ state and captures charge carriers, which is benefit to the photocatalysis process as the lifetime of photogenerated electron-hole pairs increases. After that V_O^+ will transform to V_O^0 states and V_O^{++} state, as described by the equations following:



where V_O^0 state is 0.86 eV below the CB and V_O^{++} state is 1.16 eV above the VB [53]. Upon illumination, when the catalyst is excited by photon energy greater than the band gap, electron and hole pairs are generated and electrons are trapped to the V_O^0 , releasing holes on the nanowire surface. The photo induced holes are apt to react with surface-bound H_2O or OH^- to produce the hydroxyl radical species ($^{\bullet}OH$), which is an extremely strong oxidant for the mineralization of organic pollutant. Thus the photocatalytic performances can be enhanced by modification of surface defects on the surface of the nanowire.

4. Conclusion

In summary, we have successfully prepared the zinc doped gallium oxynitride nanowires with modified surface defects via a simple electrospinning and controlled heat treatment process. With the optimized process, the obtained nanowires exhibit efficient and stable photocatalytic activity for the degradation of RhB under visible light. The apparent quantum efficiency reaches up to 30%. From the mechanism study, it is found that the surface oxygen vacancy, which serves as intermediate steps for the photocatalytic process and delays the recombination of the photogenerated electron-hole pairs, is the critical factor for controlling the photocatalytic efficiency of the nanowire. The high density of surface defects can be attributed to the effect of Zinc doping as well as ammonia treatment at high temperature. The results in this work may be beneficial to the future study of exploring the defective structure of the visible-light driven photocatalytic materials.

Acknowledgment

This study was supported by the National Natural Science Foundation of China (Grant 50872063).

Appendix A. Supplementary data

Supplementary data associated with this article can be found, in the online version, at <http://dx.doi.org/10.1016/j.apcatb.2017.03.004>.

References

- [1] A. Fujishima, K. Honda, Electrochemical photolysis of water at a semiconductor electrode, *Nature* 238 (1972) 37.
- [2] E. Bailón-García, A. Elmouahidi, M.A. Álvarez, F. Carrasco-Marín, A.F. Pérez-Cadenas, F.J. Maldonado-Hódar, New carbon xerogel-TiO₂ composites with high performance as visible-light photocatalysts for dye mineralization, *Appl. Catal. B: Environ.* 201 (2017) 29–40.
- [3] Y. Wang, J. Cheng, S. Yu, E.J. Alcocer, M. Shahid, Z. Wang, W. Pan, Synergistic effect of N-decorated and Mn²⁺ doped ZnO nanofibers with enhanced photocatalytic activity, *Sci. Rep.* 6 (2016) 32711.
- [4] Y. Zhou, G. Chen, Y. Yu, L. Zhao, J. Sun, F. He, H. Dong, A new oxynitride-based solid state Z-scheme photocatalytic system for efficient Cr (VI) reduction and water oxidation, *Appl. Catal. B: Environ.* 183 (2016) 176–184.
- [5] M. Hojaberdiel, H. Wagata, K. Yubuta, K. Kawashima, J.J.M. Vequizo, A. Yamakata, S. Oishi, K. Domen, K. Teshima, KCl flux-induced growth of isometric crystals of cadmium-containing nearly transition-metal (Ti⁴⁺, Nb⁵⁺, and Ta⁵⁺) oxides and nitridability to form their (oxy)nitride derivatives under an NH₃ atmosphere for water splitting application, *Appl. Catal. B: Environ.* 182 (2016) 626–635.
- [6] K. Maeda, T. Takata, M. Hara, N. Saito, Y. Inoue, H. Kobayashi, K. Domen, GaN:ZnO solid solution as a photocatalyst for visible-light-driven overall water splitting, *J. Am. Chem. Soc.* 127 (2005) 8286–8287.
- [7] D.P. Chen, S.E. Skrabalak, Synthesis of (Ga_{1-x}Zn_x)(N_{1-x}O_x) with enhanced visible-light absorption and reduced defects by suppressing Zn volatilization, *Inorg. Chem.* 55 (2016) 3822–3828.
- [8] W. Wei, Y. Dai, K. Yang, M. Guo, B. Huang, Origin of the visible light absorption of gaN-Rich Ga_{1-x}Zn_xN_{1-x}O_x (x = 0.125) solid solution, *J. Phys. Chem. C* 112 (2008) 15915–15919.
- [9] E.J. McDermott, E.Z. Kurmaev, T.D. Boyko, L.D. Finkelstein, R.J. Green, K. Maeda, K. Domen, A. Moewes, Structural and band gap investigation of GaN:ZnO heterojunction solid solution photocatalyst probed by soft X-ray spectroscopy, *J. Phys. Chem. C* 116 (2012) 7694–7700.
- [10] T. Ohno, L. Bai, T. Hisatomi, K. Maeda, K. Domen, Photocatalytic water splitting using modified GaN:ZnO solid solution under visible light: long-time operation and regeneration of activity, *J. Am. Chem. Soc.* 134 (2012) 8254–8259.
- [11] F. Dionigi, P. Vesborg, T. Pedersen, O. Hansen, S. Dahl, A. Xiong, K. Maeda, K. Domen, I. Chorkendorff, Suppression of the water splitting back reaction on GaN:ZnO photocatalysts loaded with core/shell cocatalysts, investigated using a μ -reactor, *J. Catal.* 292 (2012) 26–31.
- [12] K. Lee, Y. Lu, C. Chuang, J. Cistonb, G. Dukovic, Synthesis and characterization of (Ga_{1-x}Zn_x)(N_{1-x}O_x) nanocrystals with a wide range of compositions, *J. Mater. Chem. A* 4 (2016) 2927.
- [13] K. Maeda, K. Teramura, K. Domen, Effect of post-calcination on photocatalytic activity of (Ga_{1-x}Zn_x)(N_{1-x}O_x) solid solution for overall water splitting under visible light, *J. Catal.* 254 (2008) 198–204.
- [14] J. Li, B. Liu, W. Yang, Y. Cho, X. Zhang, B. Dierre, T. Sekiguchi, A. Wub, X. Jiang, Solubility and crystallographic facet tailoring of (GaN)_{1-x}(ZnO)_x pseudobinary solid-solution nanostructures as promising photocatalysts, *Nanoscale* 8 (2016) 3694.
- [15] R. Asahi, T. Morikawa, T. Ohwaki, K. Aoki, Y. Taga, Visible-light photocatalysis in nitrogen-doped titanium oxides, *Science* 293 (2001) 269.
- [16] C.C. Chen, W.H. Ma, J.C. Zhao, Semiconductor-mediated photodegradation of pollutants under visible-light irradiation, *Chem. Soc. Rev.* 39 (2010) 4206.
- [17] S.S. Chen, J.X. Yang, C.M. Ding, R.G. Li, S.Q. Jin, D.E. Wang, H.X. Han, F.X. Zhang, C. Li, Nitrogen-doped layered oxide Sr₅Ta₄O_{15-x}N_x for water reduction and oxidation under visible light irradiation, *J. Mater. Chem. A* 1 (2013) 5651–5659.
- [18] S.C. Erwin, L. Zu, M.I. HafTEL, A.L. Efros, T.A. Kennedy, D.J. Norris, Doping semiconductor nanocrystals, *Nature* 436 (2005) 91–94.
- [19] D.J. Norris, A.L. Efros, S.C. Erwin, Doped nanocrystals, *Science* 319 (2008) 1776–1779.
- [20] E.G. Seebauer, K.W. Noh, Trends in semiconductor defect engineering at the nanoscale, *Mater. Sci. Eng. R* 70 (2010) 151–168.
- [21] F. Kayaci, S. Vempati, C. Ozgit-Akgun, I. Donmez, N. Biyikli, T. Uyar, Transformation of polymer-ZnO core-shell nanofibers into ZnO hollow nanofibers: intrinsic defect reorganization in ZnO and its influence on the photocatalysis, *Appl. Catal. B: Environ.* 176–177 (2015) 646–653.
- [22] J. Wang, Y. Xia, Y. Dong, R. Chen, L. Xiang, S. Komarneni, Defect-rich ZnO nanosheets of high surface area as an efficient visible-light photocatalyst, *Appl. Catal. B: Environ.* 192 (2016) 8–16.
- [23] Y. Huang, B. Long, M. Tang, Z. Rui, M. Balogun, Y. Tong, H. Ji, Bifunctional catalytic material: an ultrastable and high-performance surface defect CeO₂ nanosheets for formaldehyde thermal oxidation and photocatalytic oxidation, *Appl. Catal. B: Environ.* 181 (2016) 779–787.
- [24] H. Wu, W. Pan, D. Lin, H. Li, Electrospinning of ceramic nanofibers: fabrication, assembly and applications, *J. Adv. Ceram.* 1 (2012) 2–23.
- [25] W. Han, Synthesis and optical properties of GaN/ZnO solid solution nanocrystals, *Appl. Phys. Lett.* 96 (2010) 183112.
- [26] D.D. Lin, H. Wu, R. Zhang, W. Pan, Enhanced photocatalysis of electrospun Ag-ZnO heterostructured nanofibers, *Chem. Mater.* 21 (2009) 3479–3484.
- [27] J. Liu, M.V. Fernández-Serra, P.B. Allen, Special quasiordered structures: role of short-range order in the semiconductor alloy (GaN)_{1-x}(ZnO)_x, *Phys. Rev. B* 93 (2016) 054207.
- [28] A. Jonotti, C.G. Van de Walle, Native point defects in ZnO, *Phys. Rev. B* 76 (2007) 165202.
- [29] B. Roul, M.K. Rajpalke, T.N. Bhat, M. Kumar, A.T. Kalghatgi, S.B. Krupanidhi, N. Kumar, A. Sundaresan, Experimental evidence of Ga-vacancy induced room temperature ferromagnetic behavior in GaN films, *Appl. Phys. Lett.* 99 (2011) 162512.
- [30] P. Boguslawski, E.L. Briggs, J. Bernholc, Native defect in gallium nitride, *Phys. Rev. B* 51 (1995) 17255.
- [31] D.G. Thoma, Interstitial zinc in zinc oxide, *J. Phys. Chem. Solids* 3 (1957) 229–237.
- [32] C.G. Zhang, W.D. Chen, L.F. Bian, S.F. Song, C.C. Hsu, Preparation and characterization of GaN films by radio frequency magnetron sputtering and carbonized-reaction technique, *Appl. Surf. Sci.* 252 (2006) 2153–2158.
- [33] K.M. Tracy, W.J. Mecouch, R.J. Nemanich, Preparation and characterization of atomically clean, stoichiometric surfaces of n-and p-type GaN (0001), *J. Appl. Phys.* 94 (2003) 3163.
- [34] M.Y. Kong, J.P. Zhang, X.L. Wang, D.Z. Sun, Hydrogen behavior in GaN epilayers grown by NH₃-MBE, *J. Cryst. Growth* 227 (2001) 371–375.
- [35] M. Chen, X. Wang, Y.H. Yu, Z.L. Pei, X.D. Bai, C. Sun, R.F. Huang, L.S. Wen, X-ray photoelectron spectroscopy and auger electron spectroscopy studies of Al-doped ZnO films, *Appl. Surf. Sci.* 158 (2000) 134–140.
- [36] A.N. Hattori, F. Kawamura, M. Yoshimura, Y. Kitaoka, Y. Mori, K. Hattori, H. Daimon, K. Endo, Chemical etchant dependence of surface structure and morphology on GaN (0001) substrates, *Surf. Sci.* 604 (2010) 1247–1253.
- [37] D. Li, M. Sumiya, S. Fukie, S. Yang, D. Que, Y. Suzuki, Y.J. Fukuda, Selective etching of GaN polar surface in potassium hydroxide solution studied by x-ray photoelectron spectroscopy, *Appl. Phys.* 90 (2001) 4219–4223.
- [38] C.L. Perkins, S.H. Lee, X. Li, S.E. Asher, T.J. Counts, Identification of nitrogen chemical states in N-doped ZnO via x-ray photoelectron spectroscopy, *J. Appl. Phys.* 97 (2005) 034907.
- [39] A.G. Marrani, F. Caprioli, A. Boccia, R. Zanoni, F. Decker, Electrochemically deposited ZnO films: an XPS study on the evolution of their surface hydroxide and defect composition upon thermal annealing, *J. Solid State Electr.* 18 (2014) 505–513.
- [40] H. Kaftelen, K. Ocakoglu, R. Thomann, S. Tu, S. Weber, E. Erdem, EPR and photoluminescence spectroscopy studies on the defect structure of ZnO nanocrystals, *Phys. Rev. B* 86 (2012) 014113.
- [41] Z.Y. Liu, D.D. Sun, P. Guo, J.O. Leckie, An efficient bicomponent TiO₂/SnO₂ nanofiber photocatalyst fabricated by electrospinning with a side-by-side dual spinneret method, *Nano Lett.* 7 (2007) 1081–1085.
- [42] Q. Wan, T.H. Wang, J.C. Zhao, Enhanced photocatalytic activity of ZnO nanotetrapods, *Appl. Phys. Lett.* 87 (2005) 083105–083107.
- [43] A. Salinaro, A.V. Emeline, J. Zhao, H. Hidaka, V.K. Ryabchuk, N. Serpone, Terminology, relative photonic efficiencies and quantum yields in heterogeneous photocatalysis. Part II: Experimental determination of quantum yields, *Pure Appl. Chem.* 71 (1999) 321–335.
- [44] I.E. Wachs, S.P. Phivilay, C.A. Roberts, Reporting of reactivity for heterogeneous photocatalysis, *ACS Catal.* 3 (2013) 2606–2611.
- [45] F. Kayaci, S. Vempati, I. Donmez, N. Biyikli, T. Uyar, Role of zinc interstitials and oxygen vacancies of ZnO in photocatalysis: a bottom-up approach to control defect density, *Nanoscale* 6 (2014) 10224–10234.
- [46] A. Bhirud, S. Sathaye, R. Waichal, C. Park, B. Kale, In situ preparation of N-ZnO/graphene nanocomposites: excellent candidate as a photocatalyst for enhanced solar hydrogen generation and high performance supercapacitor electrode, *J. Mater. Chem. A* 3 (2015) 17050–17063.
- [47] M.A. Butler, Photoelectrolysis and physical properties of the semiconducting electrode WO₃, *J. Appl. Phys.* 48 (1977) 1914–1920.
- [48] L.L. Jensen, J.T. Muckerman, M.D. Newton, *J. Phys. Chem. C* 112 (2008) 3439–3446.
- [49] M. Yoshida, T. Hirai, K. Maeda, N. Saito, J. Kubota, H. Kobayashi, Y. Inoue, K. Domen, First-Principles studies of the structural and electronic properties of the (Ga_{1-x}Zn_x)(N_{1-x}O_x) solid solution photocatalyst, *J. Phys. Chem. C* 114 (2010) 15510–15515.
- [50] B. Monemar, O. Lagerstedt, H.P. Gislason, Properties of Zn-doped VPE-grown GaN. I. Luminescence data in relation to doping conditions, *J. Appl. Phys.* 51 (1980) 625.
- [51] W.J. Moore, J.A. Freitas, G.C.B. Braga, R.J. Molnar, S.K. Lee, K.Y. Lee, I.J. Song, Identification of Si and O donors in hydride-vapor-phase epitaxial GaN, *J. Appl. Phys.* 79 (2001) 2570.
- [52] M.A. Reschchikov, H. Morkoc, Luminescence properties of defects in GaN, *J. Appl. Phys.* 97 (2005) 061301.
- [53] J.D. Ye, S.L. Gu, F. Qin, S.M. Zhu, S.M. Liu, X. Zhou, W. Liu, L.Q. Hu, R. Zhang, Y. Shi, Y.D. Zheng, Correlation between green luminescence and morphology evolution of ZnO films, *Appl. Phys. A* 81 (2005) 759–762.